香港岩土及岩土環境工程專業協會
ASSOCIATION OF GEOTECHNICAL & GEOENVIRONMENTAL SPECIALISTS (HONG KONG)
Website : www.ags-hk.org

GIG 9.0 Guidance Notes on Cone Penetration Testing

Part 2: Correlation of Geotechnical Parameters with CPT Raw Data and Application

1. Undrained Shear Strength

Correlations of the undrained shear strength S_u with the cone resistance q_c have been adopted for many years. The undrained shear strength S_u of a fine-grained cohesive soil depends on some factors like material composition, anisotropy, strain rates, stress and stress history amongst others.

There are three approaches for the interpretation of undrained shear strength with CPT as below:

- Estimation of S_u by cone resistance q_c
- Estimation of S_u by total cone resistance q_t
- Estimation of S_u by effective cone resistance q_e (I.e., $q_e = q_t - u_2$)
- Estimation of S_u by excessive pore pressure

The cone factor N_k is derived from q_c is based or theoretical approaches, and after modification and improvement, the cone factor N_{kt} derived from q_t using empirical correlation becomes more commonly adopted than other estimations. The total (Corrected) cone resistance q_t and the vertical overburden pressure (σ_{vo}) is correlated with an average undrained shear strength, S_u, by the following equation:

$$S_u = (q_t - \sigma_{vo}) / N_{kt}$$
$$= q_n / N_{kt}$$

where
S_u is the inferred undrained shear strength
q_t is the measured cone resistance
N_{kt} is an empirical bearing capacity or cone factor relating q_t to strength
σ_{vo} is the total overburden pressure
q_n is net cone resistance that is corrected cone resistance minus vertical stress

The undrained shear strength of a soil stratum could be calculated from the known q_t valve measured at a depth below the seabed. Since the unconfined compressive strength (UCS) of the soil could be obtained with soil sample from laboratory test, the correlated value of S_u from CPT can be verified by the UCS from laboratory for the cohesive soil. The equation is used to calculate S_u of the clayey stratum with the following equation:

S_u = UCS / 2 ---------- Equation 1

For the corrected q_t of a soil layer is 1,000 KPa at depth of 17m below seabed, the undrained shear strength can be calculated as follow:

$S_u = (q_t - \sigma_{vo}) / N_{kt} = (1000-17x17)/14 = 50.7$ KPa
UCS= 2 x 50.7= 101.4 KPa.

Aas et al. (1986) correlated N_{kt} with the average shear strengths from triaxial laboratory tests in compression, extension and direct shear tests. However, the cone factor must be determined empirically, from correlations based on previous investigations in the same material or correlated with insitu vane tests. Experience has shown that an N_{kt} factor in the range 10 to 18 may normally be used to give an initial estimate of shear strength (Lunne et al. (1997). Typically, N_{kt} is averagely with 14, and it tends to increase with increasing plasticity and decrease with increasing soil sensitivity. This correlation should only be confined in Zone 1, 2 3, 4 and 9 in the Normalised Soil Behaviour Type (SBTn) chart for the clay-like soil. Studies show that the value of the factor varies from 4 to greater than 30 due to some factors including sensitivity, plasticity, fissuring and possibly consolidation. Lunne et al., 1997 also showed that N_{kt} varies with pore pressure ratio B_q, where N_{kt} decreases and B_q increases, when $B_q \sim 1.0$ (i.e., sensitive clay), N_{kt} can be as low as 6.

The correlation between S_u and N_{kt} are generally conducted at specific sites in Hong Kong. The Figure 1 shows that the N_{kt} values vary from 17 to 23.5 for firm and stiff to soft clay for Chek Lap Kok Airport Project since 1997.

Summary of design parameters (Greiner-Maunsell, 1991a)

Typical Index Properties and Recommended Design Parameters	Upper Soft Clay	Stiff Clay	Firm-to-Stiff Clay	Lower Sand
Unit Weight (Mg/m^3)	1.45	1.90	1.85	2.00
Void Ratio, e_o	2.00	(2)	1.03	0.65
Maximum Past Pressure, P_p (3)	$P_p = 4.5 + 7z$	N.A.	$P_p = 55 + 15z$	N.A.
Compression Index, C_c	1.20	(2)	0.42	N.A.
Recompression Index, C_{cr}	0.10	(2)	0.085	0.03
Coeff. of Consolidation, c_v (m^2/year)	1.3	(2)	2.2	N.A.
Coeff. of Reconsolidation, c_{vr} (m^2/year)	20	(2)	15	N.A.
Undrained Shear Strength $N_k = q_{net}/S_u$ (kN/m^2)	$N_k = 23.5$	$N_k = 21.25$ (1)	$N_k = 17$	N.A.
Secondary Compression C_α	N.A.	0.3%	1.5%	N.A.

Fig 1. The designed N_k (I.e., N_{kt}) values adopted by Greiner after the series of field tests and studies in Chek Lap Kok Airport Site.

It should be noted that the N_{kt} values will not be applicable as q_c may not be measured accurately in very soft clay at shallow and intermittent depth. In addition, the use of subtraction type of CPT cone may not be appropriate for q_c measurement in very soft clay as compared with the cone type equipped with separated sensors for q_c and f_s measurements. A more appropriate method for correlation of S_u in very soft to soft soils is adopted to measure the difference of pore pressure with the following equations:

$$S_u = \frac{\Delta u}{N_{\Delta u}} \quad \text{---------- Equation 2}$$

$$N_{\Delta u} = B_q N_{kt} \quad \text{---------- Equation 3}$$

where
$\Delta u = u_2 - u_o$
$N_{\Delta u}$ = Cone factor for excessive pore pressure.

$N_{\Delta u}$ generally varies from 4 to 10. However, in lack of reliable data, the upper bound value is recommended to be selected. In order to enhance the performance of the correlation, the cone filter should be free from clogging and the cone should be fully saturated without air bubble entrapped.

The local professionals seldom adopt this method to correlate with S_u particularly in very soft clay stratum. Therefore, there are limited relevant data obtained. One of the large infrastructures in Tung Chung had acquired the test data as shown in Figure 2. Most of the $N_{\Delta u}$ results are between 8 and 13, and the average value is around 10.

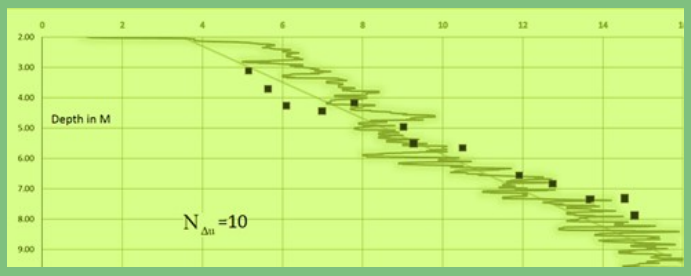

Fig. 2 Correlation of vane shear tests and excessive pore pressure with $N_{\Delta u}$ of 10.

1.1 Remoulded Undrained Shear Strengths

The remolded shear strength of soil can be obtained from vane shear test. After completion of the peak shear strength test, the vane is rotated with 12 complete revolutions to shear the soil. Then pause for 5 minutes before commencement of vane test again to find the remolded shear strength (Refer Figure 3 for details). Alternatively, the sleeve friction from the CPT testing can be used to derive the peak remolded shear strength of clay. The following equation expresses the measured sleeve friction resistance (f_s) as the remolded shear strength of clay:

$f_s \approx S_u$ (remolded)

This equation shows the lower bound value in assessing the S_u profile, and it is applicable for the SBTn in Zone 1, 2, 3, 4 and 9. The sleeve friction must be measured accurately as the remolded S_u may be as low as in between 5 to 10 KPa range.

The peak resistance strength for soil is dominantly measured from the q_c of CPT whereas the residual or the remolded shear strength is dominantly measured with f_s. The correlation test results for S_U and remolded S_u from an overseas site are manifested in Figure 4.

Fig. 3 Peak and remoulded shear strength from vane shear test

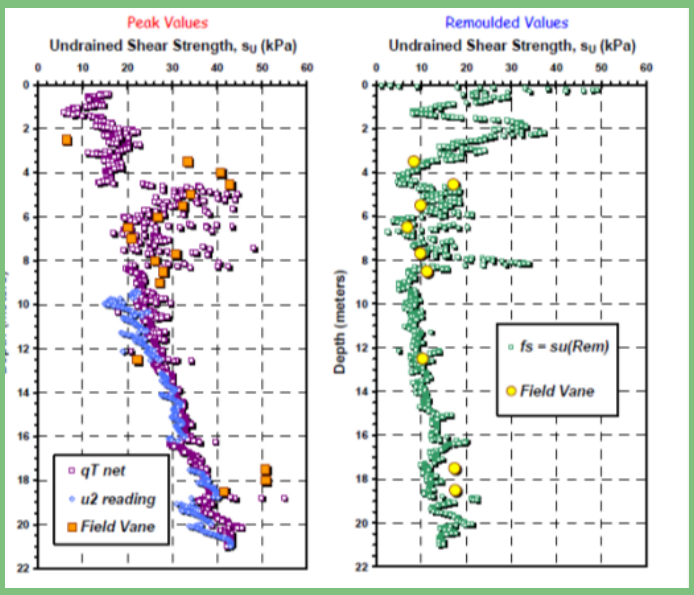

Fig. 4 Typical correlation of CPT (N_{kt} of 15 and $N_{\Delta U}$ of 10) with peak and remoulded shear strengths of field vane shear test

2. Standard Penetration Test

Standard Penetration Test (SPT) is one of the several obsolete and imperfect tests remain in common use in many parts of the world. Mayne et al (2009) correctly questions the false sense of reality in the geotechnical engineer's ability to assess each of the soil parameters from a single N-value. The geotechnical engineers should progressively abandon this crude and unreliable in-situ testing method. However, the simple operation with low cost reasonably explains that why the SPT method is used continuously in most parts of the world.

The CPT cone resistance q_c can directly be correlated to SPT N-value according to the following general linear equation:

$q_c = n\,N$, where q_c in MPa

The study from Schmertmann (1970) found that the constant, n value ranges from 0.2 for silt to sand, and to 2 for sand to sand gravel. It depends on the soil type and condition as reported from some previous studies. The study for hydraulic fill in Tung Chung by CEDD (GEO Report 42, 1977) found that the relationship between qc and N values for the overall soil profile, the marine deposit and the sandfill as shown in Figure 5. Hence, it is therefore important that the correlation for q_c and N values should be conducted specifically for large local projects.

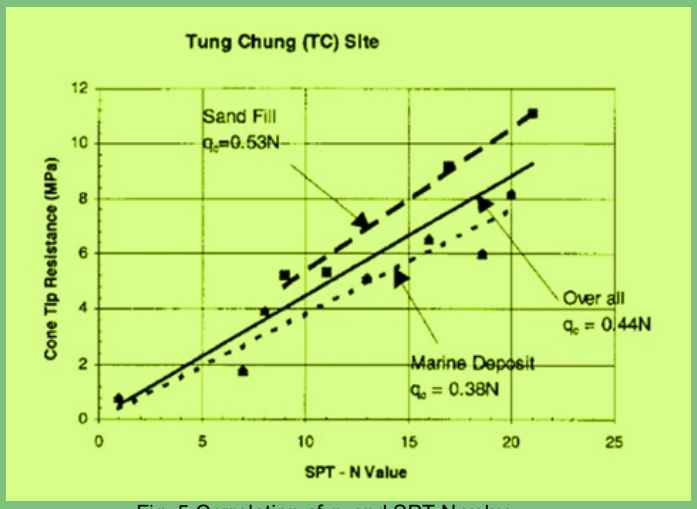

Fig. 5 Correlation of q_c and SPT N value

Many studies have been conducted to correlate SPT N values and q_c. Robertson and Campanella (1983) reviewed the correlations and presented the ratio of (q_c / Pa) / N_{60} with the mean particle size of soils (D_{50}) as shown in the Figure 6. The range of the soil D_{50} is confined from 0.001mm to 1mm.

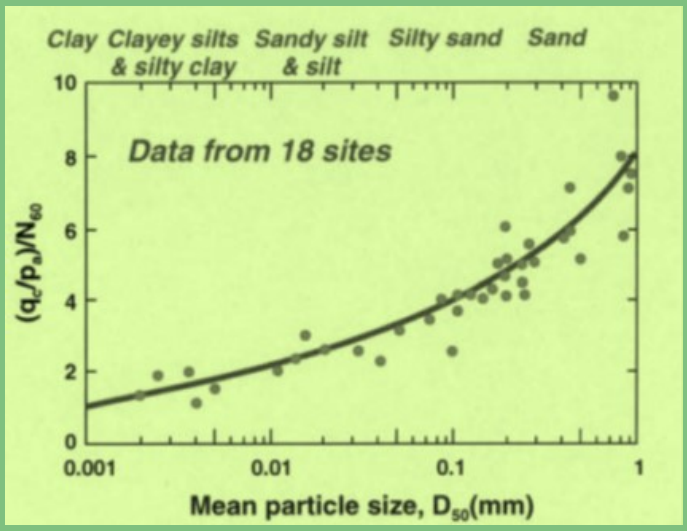

Fig.6 Correlation of modified SPT N values and D_{50} of soils

The other studies have correlated the SPT N values with CPT and fine content for sandy soils which are shown in Figure 7.

As series of laboratory tests should be conducted to get the mean grain sizes of D_{50} and fine contents for soils, it makes the correlation of SPT N values with these two parameters becomes impracticable. Besides, the correlation of CPT data with soil D_{50} is limited between 0.01 mm and 1 mm. The CPT has a trend of increasing friction ratio with increasing fines and decreasing grain size.

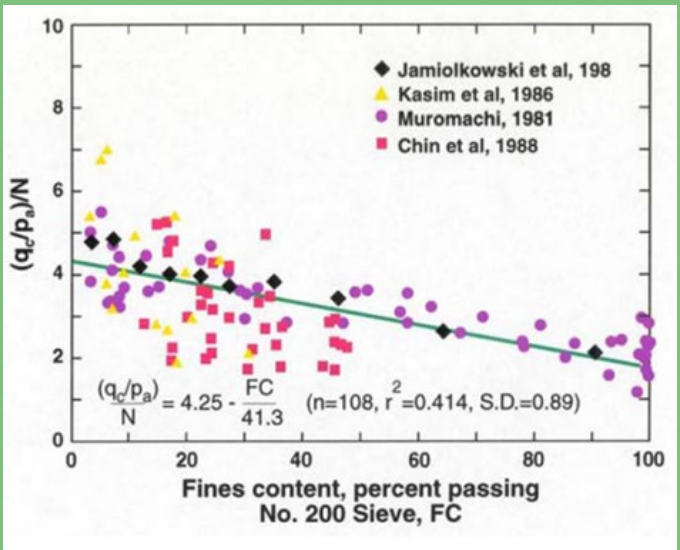

Fig. 7 Correlation of (qc / Pa) / N values and fines content for soils

Robertson et al. (1986) suggested to use the non-normalized CPT chart for (q_c / Pa) / N_{60} ratios of each soil behaviour type zone. The suggested (q_c / Pa) / N_{60} ratio for each soil behaviour type is given in Table 1. For fine grained soft soils, the correlations should be applied to total cone resistance, q_t. Note that in sandy soils, q_c = q_t.

Zone	*Soil Behavior Type (SBT)*	$\frac{(q_c/p_a)}{N_{60}}$
1	*Sensitive fine grained*	2.0
2	*Organic soils – clay*	1.0
3	*Clays: clay to silty clay*	1.5
4	*Silt mixtures: clayey silt & silty clay*	2.0
5	*Sand mixtures: silty sand to sandy silt*	3.0
6	*Sands: clean sands to silty sands*	5.0
7	*Dense sand to gravelly sand*	6.0
8	*Very stiff sand to clayey sand**	5.0
9	*Very stiff fine-grained**	1.0

Table 1. Relationship of CN and SBT Zone No.

Jefferies and Davies (1993) suggested that the most reliable method to convert the CPT cone resistance, q_t, to an equivalent SPT N value at 60% energy, N_{60}. With the soil behaviour type index, I_c, it can be combined with the CPT- SPT ratios to give the following simple relationship:

$C_{N=(}q_t$ / Pa) / N_{60} = 8.5 [1 - (I_c / 4.6)] --------- Equation 4

It should be noted that the N_{60} can be calculated based on I_c and q_t where N_{60} is defined in the following equation (Skempton 1985):

N_{60} = (ER N C_B C_S C_R) / 60 ---------- Equation 5

Where ER is the efficiency ratio of the free-fall energy for different types of SPT hammers (Refer to Table 2), and it lies between 40 and 73 by ignoring the % in the above equation. The ERs for different types of hammers are different. Some of the publications show that the ER for a fully automatic hammer may go as high as 85%.

	North America	South America	Middle East	United Kingdom	Japan	Hong Kong
Borehole Diameter (mm)		South America	100 to 150	152 to 375	65 to 110	89 to 140
Hammer Mechanism	Slip-rope, safety	Slip-rope	Automatic trip	Automatic trip	Slip-rope	Automatic trip
Average Rod Energy Efficiency(%)	45 to 60	45 to 50		73	65	?

Table 2. Summary for Energy Efficiencies for Different Types of SPT Hammers

The Constants C_B, Cs and C_R expressed in Table 3 are adjustment factors related to the borehole diameter, the sampling method adopted and the depth of SPT testing being conducted.

Factor	Equipment Variables	Value
Borehole diameter factor, C_B	2.5 - 4.5 in (65 - 115 mm)	1.00
	6 in (150 mm)	1.05
	8 in (200 mm)	1.15
Sampling method factor, C_S	Standard sampler	1.00
	Sampler without liner	1.20
Rod length factor, C_R	10 - 13 ft (3 - 4 m)	0.75
	13 - 20 ft (4 - 6 m)	0.85
	20 - 30 ft (6 - 10 m)	0.95
	> 30 ft (> 10 m)	1.00

Table 3. Correction Factors for SPT Equipment and Operation

According to the N_{60} equation from Jefferies and Davies (1993) used to correlate the soil behaviour type I_c, the ER (Energy Efficiency Ratio) for different types of SPT hammers should be known for calculation of N_{60}. However, we do not know how the authors built up the equation correctly with different ER values of different types of SPT hammers. Refer Table 3 for details.

Despite the auto-trip SPT hammers is commonly used in Hong Kong for years, it has not been calibrated in terms of the hammer energy efficiency since 1997. GEO conducted the energy efficiency test in that year. It was reported (GEO Technical Report No, 2/97, 1997) that the ER values were pin between 29% and 43%. In view of the comparably lower values of the ER found, it was concluded that further study should be conducted to find out the discrepancy. Similar ER tests were conducted by Yang W. W. (2016), and he got the ER results between

33% and 80% with the mean value greater than 60%. Phillip Chung (2018) manifested at the HKIE Geotechnical Conference in 2018 that the average ER test result from GEO"s study was found to be 68%. purpose, and further studies will be continued. It is recommended that Equation 4 delivered by Jefferies and Davis (1993) for correlation of SPT N_{60} should only be adopted in lack of reliable information and related field data from reasonable sources in your projects. Alternatively, the correlated values should be used conservatively with a higher safety factor.

3. Horizontal Coefficient of Consolidation (C_h)

For CPT carried out with piezocones, dissipation test can be performed to find the dissipation of any excess pore pressure recorded against time as presented in Figure 8. The rate of dissipation depends upon the coefficient of consolidation, which in turn, depends on the compressibility and permeability of the soil.

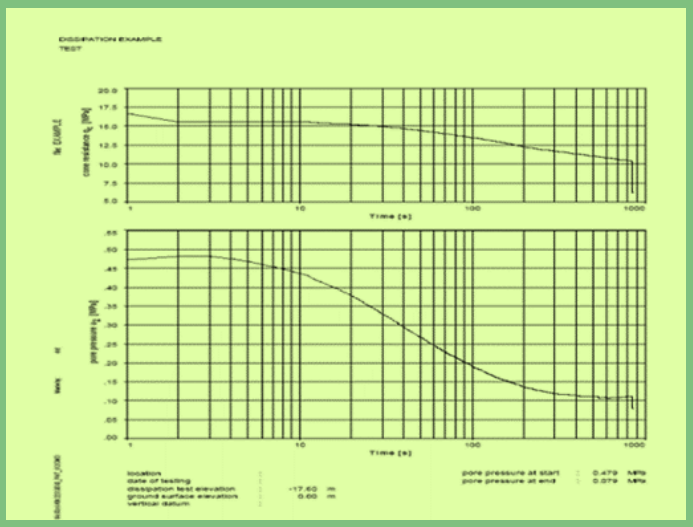

Fig 8. Plot for Dissipation Test Report

$$U = \frac{Ut - Uo}{Ui - Uo} \times 100\% \quad \text{---------- Equation 6}$$

where

u_t = pore pressure at time *t*
u_o = equilibrium pore pressure *in-situ*
u_i = pore pressure at start of dissipation test

Superimposing the Teh and Houlsby theoretical curve for dissipation over the actual curve, T* (modified time factor) can be estimated as well as the value of t. An example is given in Figure 9 for ease of reference.

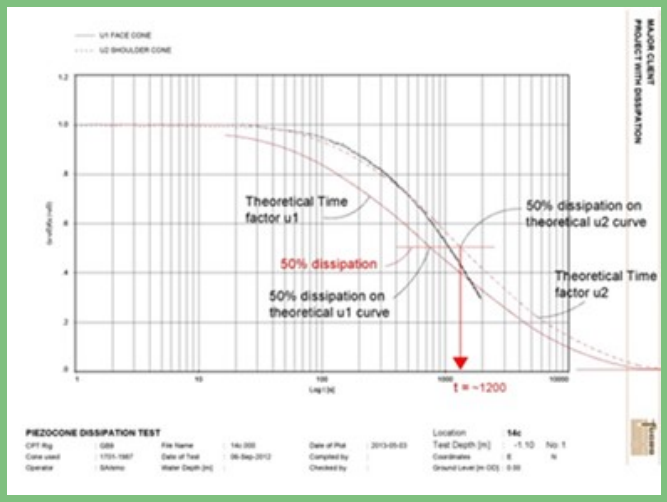

Fig 9. Dissipation Test for Determining t_{50}

From the value of the modified time factor T* it is possible to determine C_h from the following formula.

$$T^* = C_h \cdot t / r^2 \cdot I_R^{0.5} \quad \text{---------- Equation 7}$$

where

T* = Modified time factor
t = Actual time
r = Radius of CPT probe
I_R = Rigidity index = G / S_u. (Refer to Section 3.3)
C_h = Coefficient of consolidation in horizontal direction

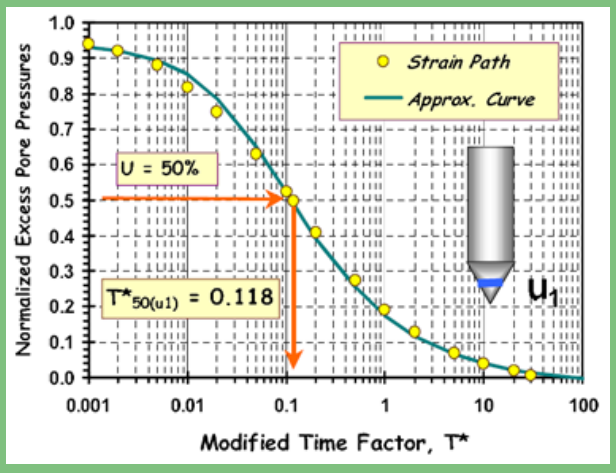

Fig 10A. Modified Time Factor for Monotonic Dissipation Test for Determining T50 for U1 Filter

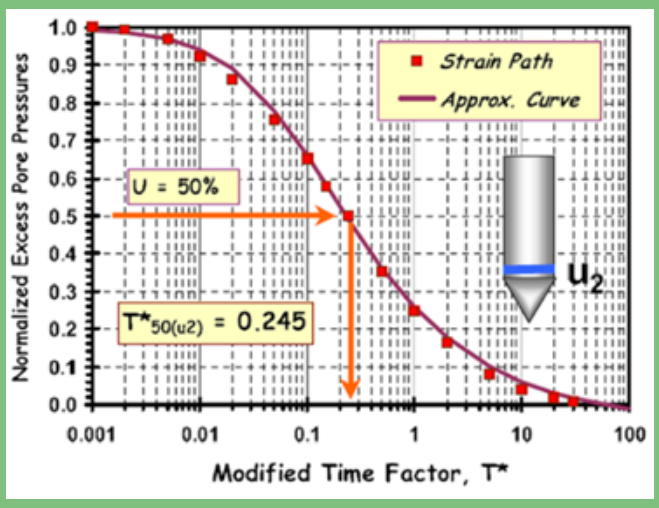

Fig 10B. Modified Time Factor for Monotonic Dissipation Test for Determining T50 for U_2 Filter

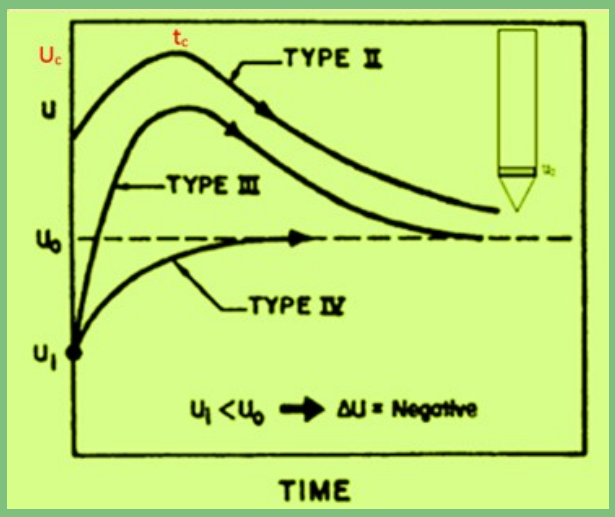

Fig.11C Type II to IV of Dilatory Dissipation

3.1 Types of Dissipation Tests

When cone penetration is halted, the induced excess pore pressure will dissipate until it reaches the hydrostatic pore pressure. A typical dissipation record shows the magnitudes of pore-water pressures monotonically decreasing with time from the initial reading. Refer to Figure 11A for details. It is similar to the behaviour of the one-dimensional consolidation test. The behaviour observed in normally to lightly overconsolidated clays when the cone filter is respectively located on the cone face (u_1), behind the shoulder (u_2), or behind the friction sleeve (u_3). However, the behaviour observed in heavily overconsolidated clays is different for u_1 but the different responses for u_2 and u_3 filters will be described under Section 4.3.

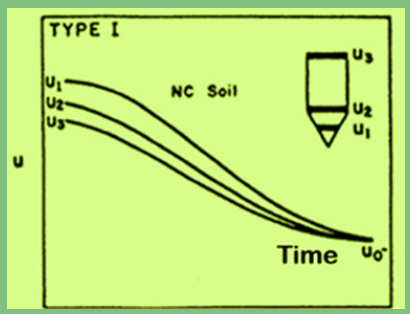

Fig.11A Type I of Monotonic Dissipation Curves

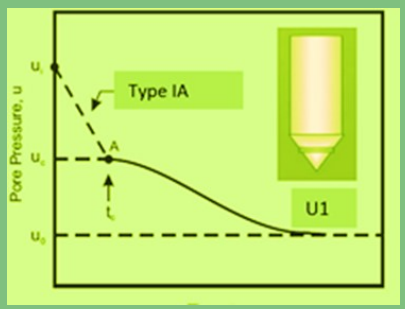

Fig.11B Type IA of Monotonic Dissipation Curves

3.2 Monotonic Dissipation (Type I and IA)

For Type 1 dissipation, the u_1, u_2 and u_3 piezocone filters always decay with time in a monotonic characteristic pattern (I.e., pore pressure decreases with time) for normally to lightly overconsolidated soils. If 50% of the normalized pore pressure is adopted, the equation is expressed as below:

$$C_h = T^*_{50}\, r^2\, I_R^{0.5} / t_{50} \text{ ---------- Equation 8}$$

where

T^*_{50} = Modified time factor at 50% of the normalized pore pressure
t_{50} = Time of dissipation at 50% of the normalized pore pressure
I_R = Rigidity index for soil

A typical calculation of C_h for Type I dissipation, the monotonic (standard) dissipation is shown in the Figure 12 and the following calculation method:

u_0= Hydrostatic pressure = 128.76KPa
u_i= Initial Pore water pressure = 579.6KPa
Dissipated pressure at 50%
= (128.76+579.6) / 2 = 354.18
T_{50}*= 0.245 for u_2 filter cone = 354.18KPa
r=1.785cm for 10cm^2 cone
$(t_{50})^{0.5}$ = 0.584
t_{50} = 0.34min
I_R=150 (Assumed)
C_h =0.245x1.7852x(150)$^{0.5}$/0.34
= 28.12 cm^2/min
= 1.47x103 m^2 / yr

It should be noted that a smaller cone, 10cm^2 cone, is used for the test, it will give you a shorter time of t_{50} when compared with the 15 cm^2 cone.

For Type1A dissipation, it should note that u_1 will exhibit a sudden drop of the initial pore pressure due to halt of penetration of the cone with unloading of cone. It is therefore important that the CPT rod should be locked during the dissipation test to avoid the sudden drop of pore pressure. The phenomenon is common for u_1 cone filter, but it is insignificant for the u_2 and u_3 filters. For calculation of C_h based on pore pressure dissipation can be considered that the time t_c (Refer to Fig. 11B) to be the initial time of dissipation and u_c be the maximum pore pressure. The normalized excessive pore pressure for dissipation should be plot against either the log time scale or the square root of time and to get the new 50% of the excessive pore pressure dissipation, $t_{50,}$ from the graph. The C_h can be calculated using the above equation.

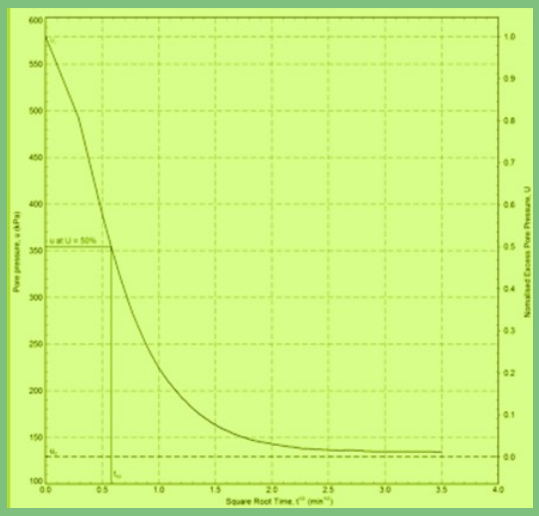

Fig. 12 Plot for Pore Pressure and Square Root Time for Monotonic Dissipation

3.3 Rigidity Index

The evaluation of rigidity index has long been considered problematic by interpretation of dissipation tests. The main difficulty in evaluating shear modulus is the variance of shear modulus with shear strain. Figure 13A illustrates shear modulus decreases with increase in shear strain. The initial shear modulus, G_{max} shown in Figure 13B typically represents the maximum tangential modulus at very low strains, while a secant modulus is used for larger strain levels and shear modulus decreases with increasing strain level. As a compromise, G_{50} suggested by Konrad & Law (1987) and Schnaid et al., (1997) is the shear modulus 50% of the mobilized strength, and it represents the average response of the soil around an advancing cone. Therefore, G_{50} is considered appropriate to be adopted for calculation of I_R.

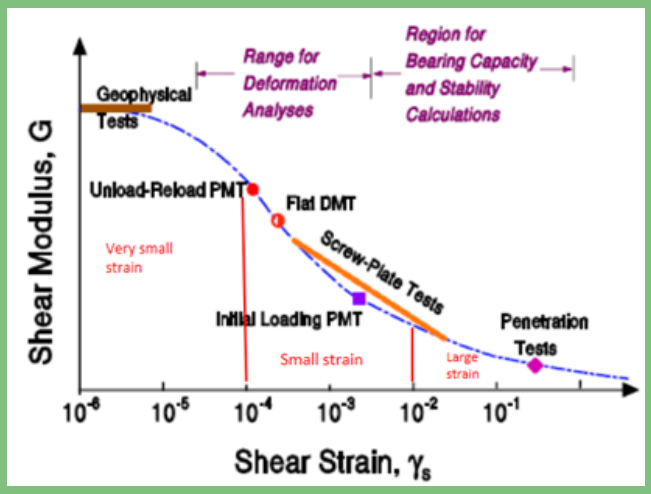

Fig. 13A Modulus Reduction Curve with Strain

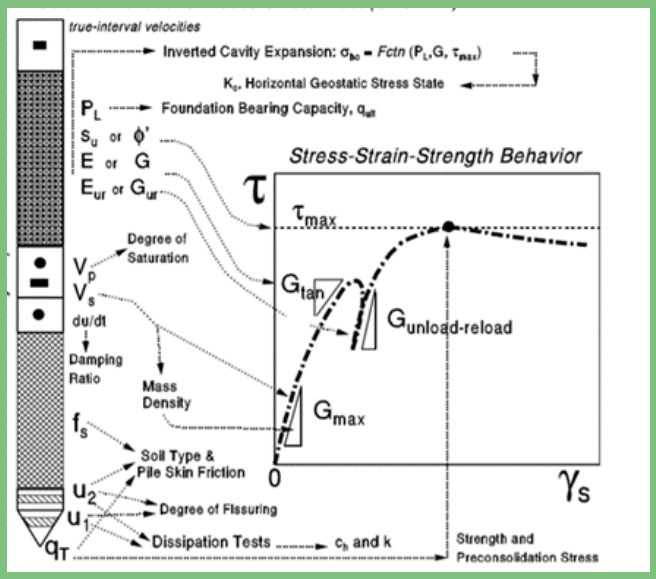

Fig. 13B Graph for Stress-Strain-Strength Behaviour Illustrates Different Shear Modulus from the Hybrid Tests of A Prospective Seismic Piezocone Pressuremeter

Keaveny and Mitchell (1986) proposed an empirical approach relating the rigidity index to the overconsolidation ratio (OCR) and clay plasticity index (PI). The methodology was based on results from triaxial CAUC test data on various clays where the I_R (I.e., I_{R50} = 50% of mobilized strength) was defined using $G_{50} = E_{50}/3$. The developed correlation can be expressed as:

$$I_{R50} \approx \frac{\exp\left(\frac{137 - PI}{23}\right)}{1 + \ln\left[1 + \frac{(OCR-1)^{3.2}}{26}\right]^{0.8}}$$ ---------- Equation 9

Figure 14 shows the relationship between the rigidity index, OCR, and PI based on Ko-consolidated triaxial compression.

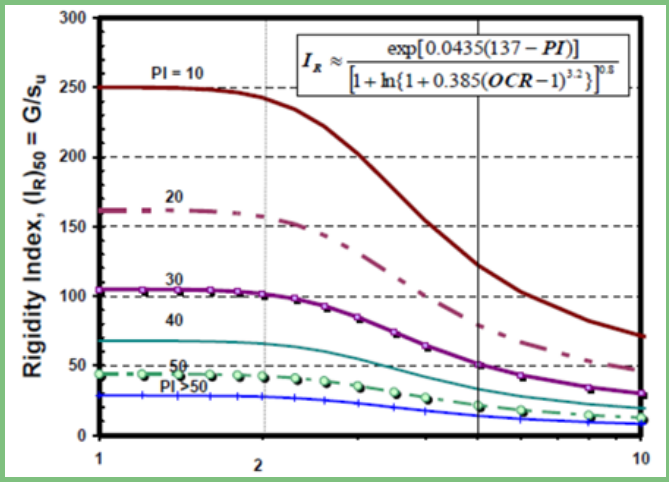

Fig. 14 Estimation of Undrained Rigidity Index of Soil from OCR and Plastic Index

The I_r varies from 20 for very highly plastic soils to 250 for low plastic soil. The maximum ratio of $I_R^{0.5}$ for the former to the latter one is 3.54, and it is generally less than half of one order of magnitude for calculating the C_h. In consideration of the difficulties in determination of C_h accurately, it is acceptable that accuracy in the estimate of the coefficient of consolidation varies within one order of magnitude (Robertson 2015).

3.4 Dilatory Dissipation (Type II and III)

In many overconsolidated and fissured materials, a dissipation test may first show an increase in pore pressure with time after a halt of penetration. Then it reaches a peak value, and decreases subsequently in pore pressure with time to hydrostatic pressure. This type of pore pressure response as shown in Figure 11C is termed dilatory dissipation. The dilatory response is observed for u_2 and u_3 filter elements during piezocone dissipation tests as well as during installation of driven piles in fine-grained soils.

Compression-induced pore pressures from increasing normal stresses are always positive; however, shear-induced pore-water pressure may be either positive (contractive) or negative (dilatant). Under the cone tip, the shear stress component can be derived from stress path analysis, which always has positive values (Chen and Mayne 1994); additionally, the magnitude of the normal-induced response is often much larger than that of the shear-induced response under the cone tip. However, along the shaft, the normal-induced and shear -induced components can be comparable in magnitude. While the normal component will always remain positive, the shear-induced component can be positive at low overconsolidation ratios (OCRs) or negative at high OCRs. The dilative dissipation curve will occur if the compression-induced pore pressure is smaller than the shear-induced pore pressure during the dissipation test.

3.4.1 Curve Fitting Method

Burns and Mayne (1998) used a model based on cavity expansion and critical-state soil mechanics theories to derive the results by a rigorous mathematical method. The solution process requires a computer program and iteration to obtain a good fit of the measured dissipation curve. During the fitting process both the horizontal coefficient of consolidation (C_h) and the rigidity index (I_R) are varied, which may be problematic and lacking a physical basis. It is not hereby to describe the method in detail due to the short cut purpose of this paper for quick application.

3.4.2 Logarithmic and Square Root of Time Methods

To account for the dilatory response, an empirical offset method was suggested by Sully and Campanella (1994) whereby the curves were shifted to the maximum value of measured pore pressure and then subjected to the monotonic decay solution.

Logarithm of Time Plot

For the u_2 filter, the maximum pore pressure, u_c, is taken as the peak value that occurs during the post-penetration increase and the time t_c at which this peak occurs is taken as the zero time of the dissipation record and all other times adjusted accordingly.

Square Root of Time Plot

The square root time plot is the most commonly used method for the dilatory dissipation. By means of extrapolating the portion of the straight line of the curve towards the ordinate to get the new value of the initial pore pressure u_c, the C_h can be calculated using the monotonic equation 8. The following typical calculation is illustrated with the plot in Figure 15:

u_0 =73.48Kpa
u_i = 240KPa
u_c= 277Kpa (Max. pore pressure from extrapolating line to Y axis)
For 50% of dissipation of the excessive pore pressure,
u_{50}= (277+73.48) / 2 = 175.24KPa
For 10 cm^2 cone with filter at shoulder (u_2 type)
T_{50}*= 0.245
r =1.785cm
t_{50} = 43.27min
I_R =120 (Assumed)

$$c_h = \frac{(T_{50}^*) r^2 \sqrt{I_R}}{t_{50}}$$ ---------- Equation 9

C_h = 0.245x1.785^{2}x (120)$^{0.5}$/43.27
= 0.198 cm^2/min
= 10.3 m2/yr

The advantage of the root-time method is that C_h can be calculated from the 50% pore pressure reduction if shorter dissipation period is used in the field and measured data for longer period is unavailable.

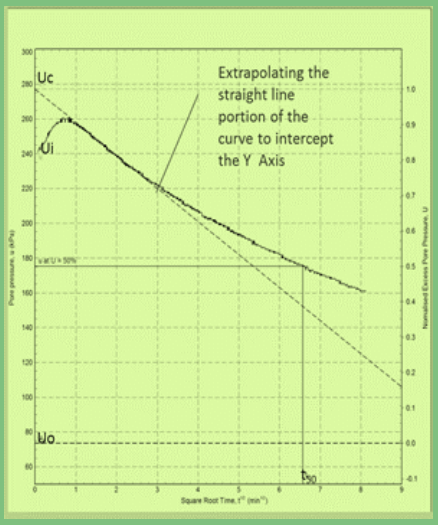

Fig. 15 Dilatory Dissipation Plot with Square Root Time Method

3.4.3 An Empirical Equation for Correcting T_{50} To T_{50m}

The corrected value of t_{50m} can be used with existing methods of test interpretation to evaluate the field value of C_h. Chen et al, (2012) proposed C_h calculation for dilatory (Non-standard) dissipation based on the numerical results. The following empirical equation is proposed to correct t_{50}:

$$t_{50m} = \frac{t_{50}}{1+18.5\left(\frac{t_{u\max}}{t_{50}}\right)^{0.67}\left(\frac{I_r}{200}\right)^{0.3}}$$ --------- Equation 10

where
t_{50m} = Corrected time for 50% excess pore pressure dissipation.
t_{50} = Time difference between the maximum and 50% of the maximum excess pore pressure (Refer to Figure 16).
t_{umax} = Time for the measured excess pore pressure to reach its maximum value.
$I_r = I_R$ = Rigidity index

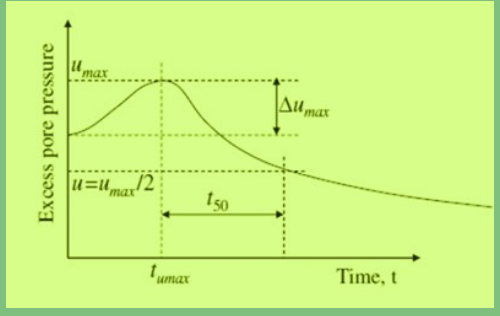

Fig. 16 Plot for t_{umax} and t50 for A Dilatory Dissipation Curve

The corrected time t_{50m} can be used to replace t50 in the equation proposed by Teh and Houlsby (1991) for standard dissipation curve to calculate directly the value of C_h with the following equation.

$$C_h = \frac{T^* \, r^2 \, (I_r)^{0.5}}{t_{50m}}$$ ---------- Equation 11

If u_2 filter is used, the equation becomes

$$C_h = \frac{0.245 \, r^2 \, (I_r)^{0.5}}{t_{50m}}$$ ---------- Equation 12

Despite the non-standard dissipation curves, C_h values evaluated by the proposed method are 2.6 to 8.8 times larger than those obtained without the t50 correction. However, the authors (Chai et al., 2021) concluded that values of C_h evaluated from the proposed method is more representative of the "true" or field values of the horizontal coefficient of consolidation than those evaluated using alternative methods.

3.4.4 Dilatory Dissipation (Type IV)

Type IV dilatory dissipation curves manifest that the initial pore pressure is negative, and it rises to the hydrostatic pore pressure but without reaching the peak pore pressure during the dissipation test. It can be considered that it is an inverse of the monotonic dissipation, and it can be treated as the standard dissipation type for calculation of the C_h.

4. Application of CPT in Deep Compaction Work

There are currently three popular deep compaction techniques to densify granular soil, namely, dynamic compaction, resonance compaction and vibroflotation (I.e., vibrocompaction). Vibroflotation is the most widely used deep compaction technique in Hong Kong attributed to many successful projects during the years. It is a process to "float" the soils by vibration to enable them to become arranged in a denser state.

4.1 Compactibility for Sandfill and CPT

Grain shape and particle size distribution play an important role in deep compaction. The silt fraction in sandy deposits should be less than 7% (Some researchers suggest the range to be between 7% and 10%) and the uniformity coefficient should be in the range from 2.2 to 6.8. Brown (1997) suggested that the granulometric curves as shown in Figure 17 with the suitability zones for vibroflotation. The soil granulometry indicates that the sandy deposit is ideally compactable in zone B and compactable in zone C.

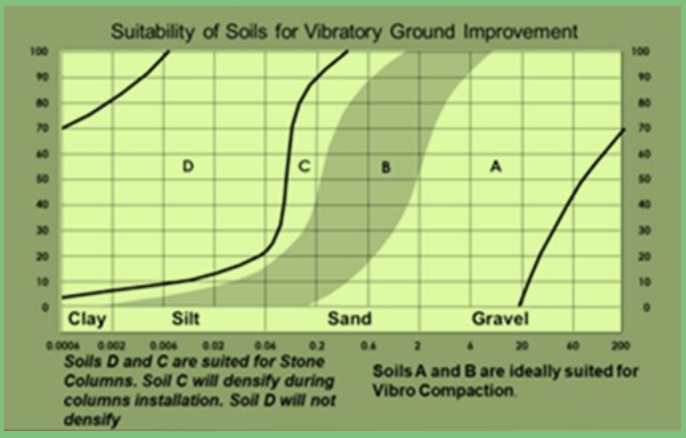

Fig. 17 Compactibility of Soil and Grain Size Distribution

In addition to the particle size distribution for soil, the increase of fines (I.e., soil particle can pass through the Sieve No 200, and the diameter of soil particles smaller than 0.074mm) will potentially inhibits the densification of soil. Figure 17 shows the broadly accepted range of grading suitable for vibroflotation. The fines content can also be exhibited in term of friction ratio on the SBT chart of q_c or q_t versus friction ratio.

Massarsch (1994) proposed an empirical relationship between cone resistance qt and friction ratio as shown in Figure 18 to assess the compatibility of soils.

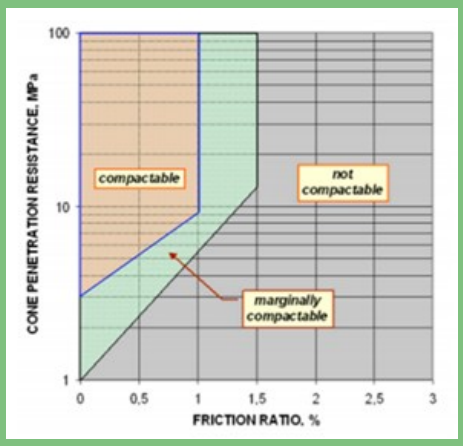

Fig.18 Classification of deep compaction and CPT Data

Soils with between 12 % silt and 30 % silt content and/ or between 1 % and 5 % clay content are difficult to judge for their compatibility.

4.2 CPT as Method of Acceptance Testing for Deep Compaction

CPT has become commonly adopted for quality control of the deep compaction because of the following reasons:

- It is fast and cost effective.
- Continuous profile with data can be acquired.
- The data obtained is reliable and repeatable.
- More parameters can be measured when compared with other in-situ tests. They include cone resistance, sleeve friction, pore water pressure and shear wave velocity if seismic cone is equipped.

It is difficult to obtain undisturbed samples of sands for laboratory testing to measure the in-situ densities directly from the deep compaction projects, CPT is then adopted to define the acceptance criteria for the reclamation projects in Hong Kong. One of the projects, the Disneyland site, specified that the qc values should achieve the designated strengths along the depth profile as shown in Figure 19A.

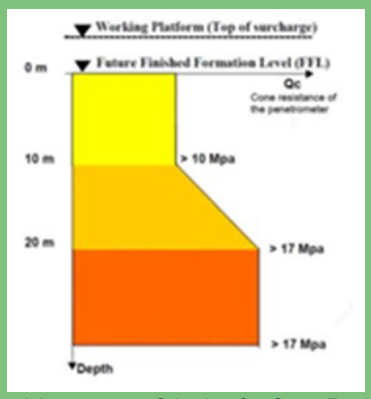

Fig. 19A Typical Acceptance Criterion for Cone Resistance q_c at Penny Bay Project

For the Central Reclamation Project Phase III in Hong Kong, it is specified that the minimum q_c criterion based on effective stress of the soils along the depth profile should be achieved (Refer to Figure 19B). If the result of any post-compaction post-CPT fails to meet the minimum specified criteria the test shall be repeated at the concerned location as directed by the Engineer. If the results of the additional testing also fail to meet the specified compliance criteria, the fills in the area shall be re-compacted and re-tested.

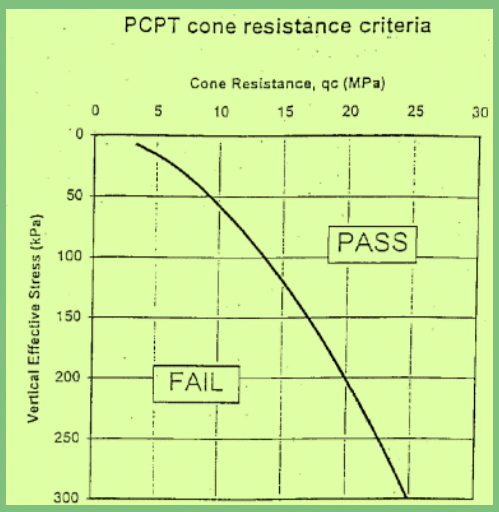

Fig. 19B The Plot for Vertical Effective Stress Vs the q_c of Post CPT for the Acceptance Criterion for Central Reclamation Project Phase III

For construction practice in Hong Kong, the deep compaction specialist contractors generally specify the limits of application for deep vibrocompaction technique based on some of the technical research and their past experiences.

In the Central Reclamation Project, Vibroflotation Group specified that fine content of soil for reclamation should not be greater than 10% and the friction ratio should not be greater than 0.8 %. Some of the projects in Asia from Keller Group generally specifies that the fine content and friction ratio should not be greater than 15% and 1% respectively.

4.3 Relative Density and CPT

The measurement of change in relative density (D_r) is also commonly adopted as the quality control (QC) criterion. However, D_r does not always well link with soil behaviour especially in sandy soils with high fines content. Besides, it can vary considerably with grain mineralogy and characteristics. Current methods of using CPT measurements for QC for deep compaction often apply only to clean silica sands and are ineffective in soils with higher fines content (Robertson, 2016). There are considerable amounts of publications that demonstrate the unreliability of relative density as an acceptance criterion. The improper estimation of the sand compressibility can produce the uncertainty in the evaluated relative density up to 20%. However, it is still adopted commonly by geotechnical professionals due to its simple application.

The definition of relative density is as below:

$$D_r = \frac{e_{max} - e}{e_{max} - e_{min}} \times 100\% = \frac{\gamma_{d\,max}}{\gamma_d} \times \frac{\gamma_d - \gamma_{d\,min}}{\gamma_{d\,max} - \gamma_{d\,min}} \times 100\%$$

---- Equation 13

where
e_{min} = void ratio of soil in densest condition
e_{min} = void ratio of soil in loosest condition
e = In-place void ratio
$\gamma_{d\,max}$ = Dry unit weight of soil in densest condition
$\gamma_{d\,min}$ = Dry unit weight of soil in loosest condition
γ_d = In-place dry unit weight

For clean sand less than 15 percent fines content, it is common practice to assess the relative density (Dr) by in-situ tests. The recent re-examination of a large Calibration Chamber Test data by Jamiolkowski, et al. (2001) which incorporates a correction factor has found that a mean relationship in terms of corrected cone tip stress can be expressed by the following equation, and the effects of relative sand compressibility can be considered by reference to Figure 20A.

$$D_R = 100 \cdot \left[0.268 \cdot \ln\left(\frac{q_t / \sigma_{atm}}{\sqrt{\sigma_{vo}' / \sigma_{atm}}} \right) - 0.675 \right]$$

---- Equation 14

where σ_{atm} = Pa = Atmospheric pressure
$D_R = D_r$

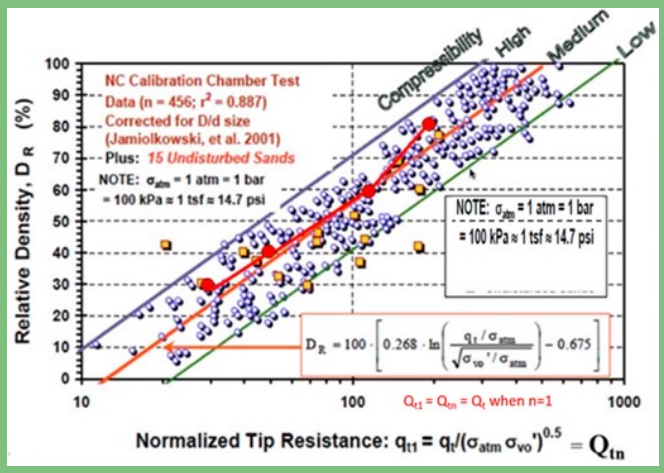

Fig. 20A Relationship Amongst Relative Density, Corrected Cone Resistance and Sand Compressibility from Corrected Chamber Test Results

One of the acceptance criteria for the performance of deep compaction works at Central Reclamation Site is based on the achievement of relative density of greater than 80% after the deep compaction work. However, it is shown in Figure 20B that part of the post treated zone at shallow depth is failed to achieve the requirement, and therefore, remedial work by means of re-compaction should be conducted.

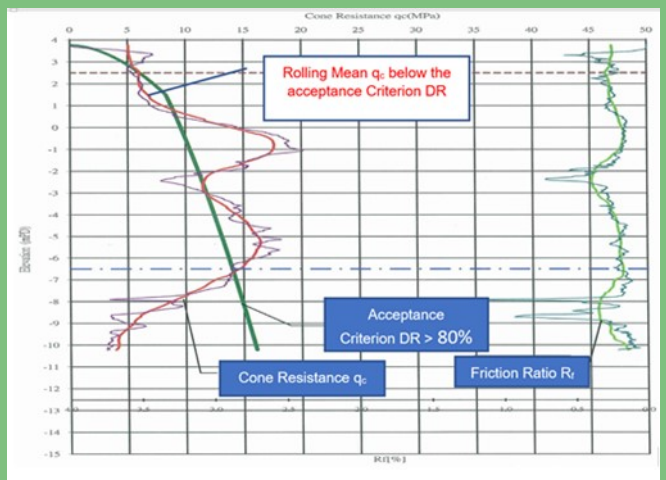

Fig. 20B Plot of Acceptance Criterion qc at Relative Density Profile of 80% Vs Actual and Rolling Mean of Post-CPT qc and Rf (From Central Reclamation Phase III)

4.4 Change in I_c for Compaction Works

The data from the site, Port of Los Angeles Phase II shows that the CPT behaviour type index I_c shifts towards a smaller number after deep compaction work. The majority of the points in Figure 21 were transformed from area 6 to 7. It seems that the soil became coarser in grain size after compaction work which of course not. The soil granulometry remains the same after vibrocompaction, and this shift of the points can be partially attributed to the increase in relative density.

I_c has not been used as one of the criteria for acceptance test for the deep compaction works. As analysis of soil type behaviour using the classification charts with additional soil type behaviour index I_c, it provides better and more comprehensive approach to the soil improvement. The Figure 22 shows that the Ic values for the soil are reduced from values to lower values after the deep compaction and the improvement factors could be assessed. Therefore, it is suggested that in future vibrocompaction projects the plotting of q_c over I_c should become a routine process by which the soil compatibility can be analysed much better.

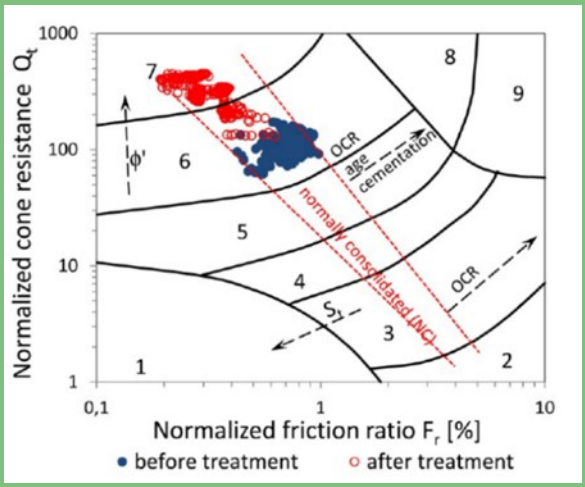

Fig. 21 Shift of I_c Before and After Deep Compaction

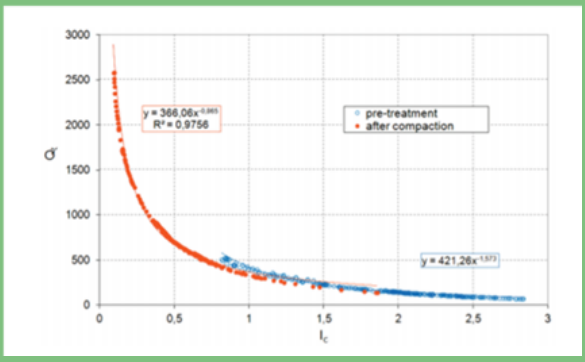

Fig. 22 Plot of Normalized Cone resistance Q_t vs Soil Behaviour Type Index I_c

5. Application of CPT in Deep Cement Mixing Work

5.1 Calibration of CPT and Torque of A Cutter Soil Mixer

Before commencement of the deep mixing work, the q_t or q_c has been to be used to calibrate with torques and pressures at the left and right rotating soil cutting drums during a trial test with CPT penetration.

For example, a deep mixing panel record from one of the local infrastructure projects as shown in Figure 23, indicates that the two rotating drums (I.e., the cutter mixers) reached the hydraulic pressures of 280 bars and 270 bars respectively at level of -17.37mPD, and maintained the pressures of greater than 100 bars for more than 10 seconds. Since it has been calibrated before in trial, the hydraulic pressure of 100 bars from the rotating drums is equivalent to the q_t value of 1.2 MPa. The drums have sustained the hydraulic pressures which are higher than the designed top level of the competent stratum with the q_t value of 1MPa. After confirming the top level of the above competent stratum has reached with satisfaction in q_t value, the cutter mixers should further penetrate 2m to terminate level as the designed toe level of the panel.

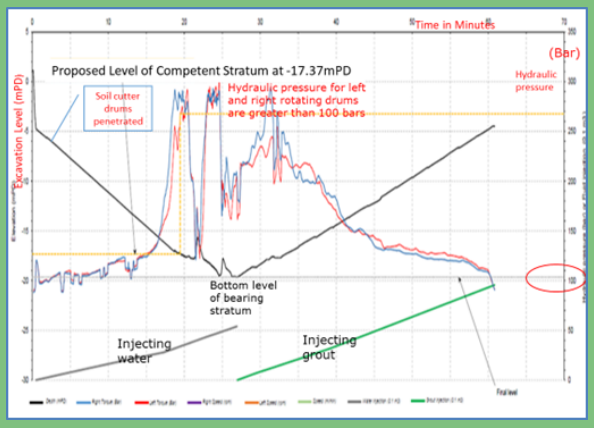

Fig. 23 Plot of Penetration of Soil Cutters in Depth with Related Hydraulic Pressures that Calibrated Before Deep Mixing Work

5.2 Determination of Toe and Bottom Levels of Competent Stratum of Deep Mixing Column

The total cone resistance q_t is frequently be used in marine infrastructures in Hong Kong to determine the bearing stratum level for the marine deep mixing work. For one of the local infrastructure projects, it is specified in the contract required CPT profile (q_t_c values), as shown as the red line profile at Figure 24, should be based on the following requirements:

1. For depth of the CPT shallower than 15m below seabed level (msbl), the corrected q_t should be greater than 1,000 KPa.

2. For depth of greater than 15mbl, the corrected q_t valve should be greater than 210+56z KPa, where z is the depth below the seabed level

The raw data q_c values are transformed into q_t values, and then calculated with filtering, shortening, and smoothing methods to get the q_t_r values (Representative CPT profile). The trail for the potential top level of the competent stratum should be checked such that q_t_r values should be greater than 90% of the q_t_c vales and the q_t_r values should be greater than 80% of q_t_c along 2m below the potential top level. After that, the data should be further adjusted and assessed with several procedures specified in the appendix of the contract specification under one of the local projects to determine the top and bottom of the competent bearing stratum of a deep cement mixing column.

It should note that the raw data qc values have been used directly to calculate and assess the competent stratum for the column in spite of approaching with correlated geotechnical parameters from CPT. For foundation design by means of using CPT values, the direct approach is commonly adopted by using the q_c and f_s to find the bearing capacity and friction of a soil stratum. One of the direct approaches, the LCPC method introduced by Bustamante and Gianeselli (1982), is commonly adopted for calculating the allowable bearing capacity for the deep foundation. It is uncommon and might be more complicated to approach through correlation of geotechnical parameters.

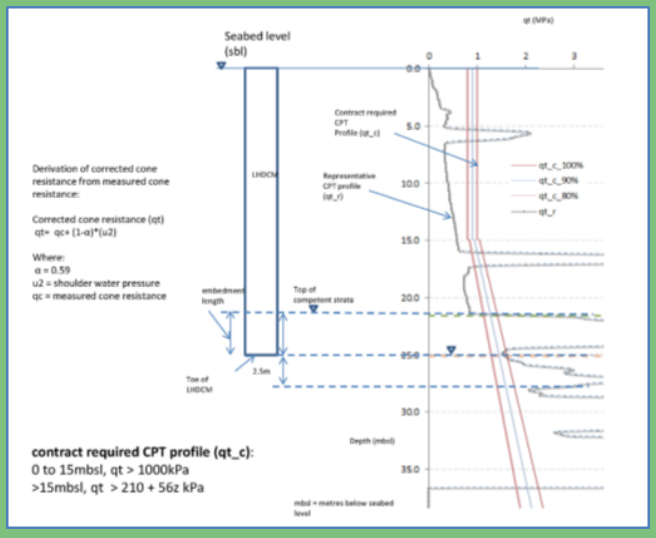

Fig. 24 Termination Criterion of CPT for Bearing Strata of A Deep Cement Mixing Project

6. Abbreviation and Symbols

Standard Cone Measurements and Factors

pwp	Pore water pressure
q_c	Measured cone end resistance
α	Cone shaft face to face ratio
β	value of excessive pwp cone ratio- 0.8 for the face (u_1) and 1.0 on the shoulder (u_2)
u_o	Theoretical hydrostatic pwp relative to ground level acting on cone.
u_1	Measured pwp at cone face elevation
u_2	Measured pwp at cone shoulder
u_3	Measured pwp behind cone sleeve tube

Pressures

σ_{vo}	Total overburden ground pressure
σ_{vo}'	Effective overburden ground pressure
σ_{atm}	Atmospheric pressure (Pa)

SBT Soil Bar Type

q_t	Total cone end resistance corrected for pwp effect where $q_t = (1-\alpha).(u_0 + \beta(u_2-u_0))$
q_n	Net cone end resistance where $q_n = q_t-\sigma_{vo}$
σ_{atm}	Atmospheric pressure (Pa)

Normalised Parameters

SBTn	Normalized Soil Bar Type
Q_t	= Normalized cone resistance $= ((q_t- \sigma_{vo}) / \sigma_{vo}')$
F_r	Friction Ratio= $f_s / (q_t- \sigma_{vo})$
B_q	Pore Pressure Ratio = fs / (qt- σvo)

Updated Normalized Parameters

Q_{tn}	Normalized net cone resistance $= ((q_t- \sigma_{vo}) / P_a) . (P_a / \sigma_{vo}')^n$
n	= Stress Exponent factor where n=1 for clay n=0.5 for sand

7. References

Aas, G., Lacasse, S., Lunne, T. and Hoeg, K. (1986).

Use of Insitu Tests for Foundation Design on Clay. Proceedings of the ASCE Speciality Conference Instu 86, ASCE.

ASTM D5778-12, (2012). Standard Test Method for Performing Electronic Friction Cone and Piezocone Penetration Testing of Soils, ASTM International.

Brown, R.E. (1997) Vibroflotation Compaction of Cohesionless Soils. Journal of the Geotechnical Engineering Division, 103(12):1437–1451.

BSI, (2012). Geotechnical Investigation and Testing – Field Testing, Part 1: Electrical Cone and Piezocone Penetration Test (BS EN ISO 22476-1:2012), British Standards Institution, London, 46 pp.

Begemann H. K. S. P. H. (1953), Improved in Determining Resistance to adhesion by Sounding through a Sleeve Loose Placed Behind the Cone, Proceeding 3rd ICSMFE Zurich, Switzerland, Vol. 1, Page 213-217.

Burns and Mayne(1998). Canadian Geotechnical Journey Vol 35: 1063–1073

Bustamante and Giasenelli 1982. Pile Bearing Capacity Prediction by Means of Static Penetrometer CPT. Proceedings of the Second European Symposium on Penetration Testing, ESOPT-II, Amsterdam, 2 493-500.

CEDD (1977). GEO Technical Report 42.

CEDD (1997). GEO Technical Report No, 2/97

CHAI et al., (2014), Coefficient of Consolidation from Piezocone Dissipation Tests, Proceedings of the International Symposium on Lowland Technology, September 2004.

Chai J. C. et al., (2021), Coefficient of consolidation from non-standard piezocone dissipation curves, Computers and Geotechnics 41 (2012) 13–22.

Chen, B.S.Y., and Mayne, P.W. (1994). Profiling the over-consolidation ratio of clays by piezocone tests. Georgia Institute of Technology, Atlanta, Internal Report GIT-CEEGEO-94-1.

Keaveny, J. and Mitchell, J.K. (1986). Strength of fine-grained soils using the piezocone. Use of In-Situ Tests in Geotechnical Engrg. (GSP 6), ASCE, Reston/VA, 668 -685

Konrad, J.M., and Law, K.T., (1987). "Undrained shear strength from piezocone tests." Can. Geotech. J., 24,

IRTP, (1999). Technical Committee TC16, ISSMGE, "International Reference Test Procedure for Cone Penetration Test (CPT) and the Cone Penetration Test with Pore Pressure (CPTU)", Proc., the XIIth ECSMGE, Amsterdam, Balkema, 2195-2222.

Jamiolkowski, M., D.C.F. LoPresti, and M. Manassero, (2001). "Evaluation of Relative Density and Shear Strength of Sands from Cone Penetration Test and Flat Dilatometer Test," *Soil Behavior and Soft Ground Construction* (GSP 119), American Society of Civil Engineers, Reston, Va., 2001, pp. 201–238.

Jefferies, M.G., and Davies, M.P., (1993). Use of CPTU to mate equivalent SPT N60. Geotechnical Testing Journal, ASTM, 16(4): 458–468.

Lunne, T., Robertson, P.K., and Powell, J.J.M. (1997). Cone Penetration Testing in Geotechnical Practice. Blackie Academic/Routledge Publication, New York, 312 pp.

Meigh. A. C. (1987). CIRIA Ground Engineering Report: In situ testing. Cone Penetration Testing, Methods and Interpretation.

Massarsch, K.R., (1994). Settlement Analysis of Compacted Fill. Proceedings, 13th International Conference on Soil Mechanics and Foundation Engineering, ICSMFE, New Delhi, Vol. 1

Mayne 2009

Robertson, P.K., Campanella, R.G., Gillespie, D., and Rice, A., (1986). Seismic CPT to measure in-situ shear wave velocity. Journal of Geotechnical Engineering Division, ASCE, 112(8): 791–803.

Robertson, P. K., (1990). Soil Classification Using CPT: Canadian Geotechnical Journal. Vol.27, No. 1, pp151-158.

Robertson, P.K. and Wride, C.E., (1998). Evaluating cyclic liquefaction potential using the cone penetration test. Canadian Geotechnical Journal, Ottawa, 35(3): 442 –459.

Robertson P. K and Cable (Robertson) K.L., (2012). Guide to cone Penetration Testing for Geotechnical Engineering, Gregg Drilling and Testing Inc., 5Th Edition.

P.K. Robertson (2016). Geotechnical and Geophysical Site Characterisation 5 – Lehane, Acosta-Martínez & Kelly (Eds) © 2016 Australian Geomechanics Society, Sydney, Australia, ISBN 978-0-9946261-1-0

Schmertmann, J. H. (1970) Static cone to compute static settlement over sand, ASCE, Journal of the Soil Mechanics and Foundations Division. 96 (3), 1011-1043.

Sully and Campanella (1994). An approach to evaluation of field CPTU dissipation data in overconsolidated fine-grained soils: Discussion. Canadian Geotechnical Journal

Teh, C.I., Houlsby, G.T. (1991). An analytical study of the cone penetration test in clay. Geotechnique 41

YANG Wenwei. 2006) Doctorate Thesis, The University of Hong Kong.

Zhang, G., Robertson, P.K., and Brachman, R.W.I., 2002, Estimating Liquefaction induced Ground Settlements from CPT for Level Ground, Canadian Geotechnical Journal, 39(5): 1168–1180.